



Preparation, characterization and biological evaluation of β -cyclodextrin-biotin conjugate based podophyllotoxin complex

Xiu Zhao^a, Neng Qiu^{a,*}, Yingyu Ma^a, Junda Liu^a, Lianying An^a, Teng Zhang^a, Ziqin Li^a, Xu Han^a, Lijuan Chen^b

^a Department of Chemical & Pharmaceutical Engineering, College of Materials and Chemistry and Chemical Engineering, Chengdu University of Technology, Chengdu 610059, China

^b State Key Laboratory of Biotherapy and Cancer Center, West China Hospital, West China Medical School, Sichuan University, Chengdu 610041, China

ARTICLE INFO

Keywords:

β -cyclodextrins
Podophyllotoxin
Biotin
Solubility
Complex

ABSTRACT

Podophyllotoxin is a natural occurring aryltetralin lignin with pronounced cytotoxic activity. However, its clinical application for cancer treatment has been blocked due to its poor water solubility and selectivity. In this work, biotin as a tumor specific ligand was coupled with β -cyclodextrin and the resulting biotin modified β -cyclodextrin was used to complex with podophyllotoxin to improve its aqueous solubility and tumor selectivity. The solubility of β -cyclodextrin was greatly enhanced (>16 times) by conjugating with biotin. podophyllotoxin/ mono-6-biotin-amino-6-deoxy- β -cyclodextrin inclusion complex was prepared by freeze-drying method and the complex behavior between mono-6-biotin-amino-6-deoxy- β -cyclodextrin and podophyllotoxin was studied by water solubility, phase solubility, Job's plot, UV spectroscopy, Proton Nuclear Magnetic Resonance, Rotating-frame Overhauser Effect Spectroscopy, Powder X-ray diffraction and Scanning electron microscopy. The solubility of podophyllotoxin/ mono-6-biotin-amino-6-deoxy- β -cyclodextrin complex was greatly improved (9 times) compared with Podophyllotoxin. The stability constant of podophyllotoxin/ mono-6-biotin-amino-6-deoxy- β -cyclodextrin complex ($K_s = 415.29 \text{ M}^{-1}$) was 3.2 times that of podophyllotoxin/ β -cyclodextrin complex. The possible inclusion mode of podophyllotoxin/mono-6-biotin-amino-6-deoxy- β -cyclodextrin complex was inferred from the Proton Nuclear Magnetic Resonance and Rotating-frame Overhauser Effect Spectroscopy. The cellular uptake study showed that the introduction of biotin increased the cellular uptake of rhodamine-B/mono-6-biotin-amino-6-deoxy- β -cyclodextrin complex. Moreover, cell cytotoxicity study showed that the antitumor activity of podophyllotoxin/ mono-6-biotin-amino-6-deoxy- β -cyclodextrin complex was more potent than podophyllotoxin/ β -cyclodextrin complex and free podophyllotoxin. The superior water solubility and enhanced cytotoxicity suggested that the mono-6-biotin-amino-6-deoxy- β -cyclodextrin associated inclusion complex might be a potential and promising delivery system for hydrophobic chemotherapeutics such as podophyllotoxin.

1. Introduction

Podophyllotoxin, a lignan derived from *podophyllum species*, has shown to possess various types of pharmaceutical activity such as anthelmintic (Wang et al., 2015), antifungal (Anil Kumar et al., 2007), antiviral (Gong et al., 2019) and antineoplastic (Gordaliza et al., 2000). Previous reports have demonstrated that PPT and its derivatives including etoposide and teniposide have been successfully utilized to treat lung cancer, liver cancer, breast cancer, non-Hodgkin and other lymphomas (Giri and Narasu, 2000; Yu et al., 2017). The mechanism of

the anti-cancer activities of PPT are mainly attributed to binding of the colchicine site of tubulin, disrupting microtubule assembly, which results in mitotic arrest and cellular apoptosis (Imbert, 1998; Roy et al., 2017). However, the systemic application of PPT for the treatment of cancer has been greatly limited due to the poor water solubility and lack of selectivity. Therefore, it is of critical importance to develop a treatment strategy that is able to improve the aqueous solubility and selectivity of PPT.

The use of delivery system to improve the water solubility of lipophilic drugs has been explored during the past several decades. Among

* Corresponding author.

E-mail address: qiuneng168@163.com (N. Qiu).

<https://doi.org/10.1016/j.ejps.2021.105745>

Received 12 October 2020; Received in revised form 2 January 2021; Accepted 1 February 2021

Available online 5 February 2021

0928-0987/© 2021 Elsevier B.V. All rights reserved.

those delivery system, cyclodextrin (CD) complexation has become the focus of interest for hydrophobic drug delivery due to its reliable safety profile, simple preparation method and high drug loading capacity. Cyclodextrins (CDs) are cyclic derivatives of starch that is obtained from starch by enzymatic process (Hädärugä et al., 2019). They are torus shaped circular α -(1,4) linked oligosaccharides that have been extensively used to improve the aqueous solubility, bioavailability and stability or decrease unfavorable side effects of drugs (Periasamy et al., 2020; Carmen et al., 2005; Liu et al., 2003). A unique conical structure with hydrophobic cavity is formed by the glucose chains in CDs, and lipophilic compounds may enter and form water-soluble complexes that alter the physical and chemical properties of drug (Gould and Scott, 2005). α -, β - and γ -CD consist of six, seven and eight glucose units respectively, are the most studied cyclodextrins. In particular, β -CD is more extensively used in drug delivery systems due to the appropriate cavity size, good ability to combine aromatic units, ready availability, easy production, and relatively economical price (Stappaerts et al., 2018; Liao et al., 2015; Waleczek et al., 2003; Yao et al., 2014). However, the low water solubility (1.85g/100ml) of parent β -CD limits their further application in pharmaceutical formulations (Periasamy et al., 2020; Qiu et al., 2017). The relatively low water solubility of β -CD may be owing to an internal hydrogen bond formed between the C-2-OH and the C-3-OH of the neighboring glucose unit. The formation of the hydrogen bond in the β -CD molecule result in a secondary belt, leading to a rather rigid structure (Qiu et al., 2017). In addition, β -CD application is also limited due to the lack of selectivity. The development of site-specific delivery system with greater efficacy and lower toxicity is recently an urgent need to overcome the limitation of conventional therapy.

Biotin, one of the B vitamins, also known as vitamin H, is a water-soluble vitamin. As a cellular growth promoter, biotin and its derivatives have already been used in the field of cancer studies and tissue engineering (Na et al., 2003). Biotin was found in kidney, liver, pancreas and milk (Park et al., 2006). Due to the rapid cell growth and enhanced proliferation, cancer cells need more certain vitamins than normal cells. Therefore, the receptors involved in the uptake of vitamins are usually overexpressed on the surface of tumor cells and as a consequence these surface receptors are useful as tumor-targeting biomarkers. It has been reported that additional biotin is needed for the rapid growth and proliferation of cancer cells (Bian et al., 2012). Specifically, biotin is present in higher content in cancerous tissue than in normal tissue (Bagheri et al., 2014). Coincidentally, biotin receptors have been reported to be over-expressed on the surfaces of many types of tumor cells (Yan et al., 2019). Highly proliferating cancer cells such as MDA-M231, MCF7, A549, HeLa and HepG2 cells exhibit elevated biotin receptors in comparison with health cells. Therefore, biotin is a popular targeting agent for drug delivery system. As a specific active targeting agent (Lammers et al., 2008), biotin has been utilized in drug carriers to increase intracellular uptake of drug and decrease toxicity in normal tissues (Bagheri et al., 2014). When biotin conjugated with other drug via amide or ester linkages, it spontaneously acts as a targeting moiety for specific interaction with tumor cells (Park et al., 2006). Previous report demonstrated that a biotin and arginine modified hydroxypropyl- β -cyclodextrin could improve the anticancer activity of paclitaxel (Yang et al., 2019). Therefore, we hypothesized that biotin as a tumor specific ligand conjugated with β -CD to improve its cancer selectivity is feasible.

The purpose of this study is to improve the water solubility and cancer selectivity of the PPT through the formation of PPT/ β -CD inclusion complexes. The inclusion complexes of PPT/ β -CD were prepared and analyzed by water solubility, phase solubility, Job's plot, ^1H NMR and 2D ROESY NMR, Powder X-ray diffraction (XRD), Fourier transformation-infrared spectroscopy (FT-IR), Scanning electron microscopy (SEM). In addition, the cell cytotoxicity experiment was conducted to study the antitumor activity of the PPT/ β -CD complexes. The cellular uptake was carried out to investigate the targeting ability of β -CD with rhodamine B as a fluorescence probe.

2. Materials and methods

2.1. Materials

β -CD (99.0%, MW=1135.00) and *p*-toluenesulfonyl chloride were purchased from Chengdu Kelong Chemical Co., Ltd. (Chengdu, China). Biotin was obtained from Shanghai Duoduo Chemical Industries Co Ltd. (Shanghai, China). Podophyllotoxin (98%) was obtained from Shanghai Yuanye Bio-Technology Co., Ltd. (Shanghai, China). Triphenylphosphine was obtained from Tianjin Kemiou Chemical Reagent Co., Ltd. (Tianjin, China). All other chemical reagents were of analytical grade and all materials were used according to the instructions.

2.2. Chemical synthesis of mono-6-biotin-amino-6-deoxy- β -cyclodextrin (β -CD) (Fig. 1)

Synthesis of mono-6-(*p*-toluenesulfonyl)-6-deoxy- β -cyclodextrin (β -CD-OTs): β -CD-OTs was synthesized according to a previously reported method (Abbas et al., 2017). Generally, β -CD (5g, 4.4mmol) was suspended in 30 ml of ultra-pure water. Sodium hydroxide (8M, 1.75ml) was added dropwise until the β -CD solution was clarified. A solution of *p*-toluenesulfonyl chloride (1g, 5.28mmol) in 2.5 ml of acetonitrile was added dropwise to the β -CD solution under vigorous stirring in an ice water bath at 0-5°C. Then hydrochloric acid (2M) was added to the neutralize the solution. After stirring at 25°C for 2h, a large amount of white precipitate was formed. Then the resulting precipitate was collected by vacuum filtration and recrystallized two or three times in hot water. The obtained white product (β -CD-OTs) was dried at 40°C under vacuum and collected as a white solid (0.9563g, 19.1%). ^1H NMR (400 MHz, DMSO- d_6): δ 7.77-7.75(d, 2H), 7.45-7.43(d, 2H), 5.82-5.63 (m, 14H), 4.86-4.77(m, 7H), 4.52-4.43(m, 6H), 3.67-3.55(m, 28H), 3.40-3.28(overlap with H₂O, m, 14H), 2.44-2.43(s, 3H). MS(ES), m/z: 1311.39[M+Na]⁺

Synthesis of mono-6-azide-6-deoxy- β -cyclodextrin (β -CD-N₃): β -CD-OTs (1g, 0.77mmol) and sodium azide (1.32g, 20.36mmol) were dissolved in 15ml of ultrapure water at 80°C. The mixture solution was stirred at 80°C for 24h. The mixture was cooled to room temperature and 70ml of acetone was poured, immediately producing a white precipitate. The resulting product (β -CD-N₃) was collected with suction filtration and vacuum dried overnight at 40°C to obtain a white powder (yield: 88%). ^1H NMR (400 MHz, DMSO- d_6): δ 5.76-5.61(m, 14H), 4.88-4.82(m, 7H), 4.51-4.42(m, 6H), 3.79-3.51(m, 28H), 3.42-3.31(overlap with H₂O, m, 14H). MS(ES), m/z: 1182.38[M+Na]⁺

Synthesis of mono-6-amino-6-deoxy- β -cyclodextrin (β -CD-NH₂): β -CD-NH₂ was synthesized in a procedure described by Wei et al (Wei et al., 2013). Briefly, β -CD-N₃ (1g, 0.86mmol) and triphenylphosphine (0.3g, 1.1mmol) were dissolved in 10 ml of N,N-dimethyl formamide and stirred for 2h at 25°C. Then 2ml distilled water was added, stirred at 90°C for 2 hours, cooled to room temperature and 20ml of acetone was poured, immediately producing a white precipitate. The white product (β -CD-NH₂) was collected by filtration and vacuum dried 60°C to obtain the desired product (yield: 92%). ^1H NMR (400 MHz, DMSO- d_6): δ 5.78-5.58(m, 14H), 4.91-4.79(m, 7H), 4.50-4.37(m, 6H), 3.76-3.48(m, 28H), 3.41-3.33(overlap with H₂O, m, 14H). MS(ES), m/z: 1134.39[M+H]⁺

Synthesis of Biotin-N-hydroxysuccinimide ester (Biotin-NHS): Biotin (97.6mg, 0.4mmol), N-hydroxysuccinimide (NHS, 48mg, 0.42mmol) and N,N'-Dicyclohexyl-carbodiimide (130mg) were dissolved in 3 ml of N,N-dimethylformamide. The reaction mixture was kept stirring in condition of seal for 3h at 55°C. The mixture was cooled to room temperature and filtrated to remove the insoluble solid. The filtrate was precipitated in diethyl ether under stirring in an ice water bath. The precipitate was collected (Biotin-NHS) by filtration and dried in the air, giving the desired product as white solid (yield: 92%). ^1H NMR (400 MHz, DMSO- d_6): δ 6.40-6.34(d, 2H), 4.32-4.29(m, 1H), 4.16-4.13(m, 1H), 3.13-3.08(m, 1H), 2.82-2.81(s, 4H), 1.69-1.38(m, 8H).

Synthesis of mono-6-biotin-amino-6-deoxy- β -cyclodextrin(B-CD). β -CD-NH₂ (1.134g, 1mmol) and Biotin-NHS(0.395g, 1mmol) were dissolved in 10 ml of N,N-dimethyl formamide and stirred for 24 h at 25°C. The mixture was cooled to room temperature and 20ml of acetone was poured, immediately producing a white precipitate. Then the white precipitate was collected by filtration and dried under vacuum at 60°C. The B-CD product was obtained as a white powder(yield:62%). ¹H NMR (400 MHz, DMSO-d₆): δ 5.84-5.71(m, 14H), 4.85-4.81(m,7H), 4.49-4.42(m, 6H), 4.32-4.29(m, 1H), 4.147-4.116(m, 1H), 3.71-3.56(m, 28H), 3.39-3.17(overlap with H₂O, m, 14H), 3.124-3.089(m, 1H), 2.85-2.80(m, 2H), 1.64-1.27(m, 8H). MS(ES), m/z:1382.46[M+Na]⁺

2.3. Phase solubility studies

The method described by Higuchi and Connors was used to study the phase solubility of PPT and B-CD (Waleczek et al., 2003; Sifaka et al., 2016). Briefly, excessive podophyllotoxin was added to aqueous solution of B-CD (ranging from 0 to 10 mM) and stirred for 24h at 37°C. Then the mixture solution was centrifuged at 3500 rpm for 10 min and the supernatant was removed. Then the concentration of PPT was analysed by UV Spectrophotometer at 291 nm. The phase solubility diagram was obtained by plotting the relationship between PPT and the concentration of B-CD.

2.4. Job's plot

The Job's plot was obtained by using the UV Spectra. Briefly, the PPT and B-CD were dissolved in the mixture solution of water and ethanol. The total molar concentration of PPT and B-CD remained unchanged at 2.5×10^{-4} M and the molar ratio of PPT ($R = \text{PPT}/[\text{PPT}] + [\text{B-CD}]$) was varied from 0.0 to 1.0. After using laboratory shaker for 24h at 37°C, the UV Spectra absorbance data was recorded at 291 nm and the absorption of PPT solution were obtained in the presence and absence of B-CD under the same condition.

2.5. Preparation of PPT/B-CD inclusion complex

Freeze-drying method was developed to prepare PPT/B-CD inclusion complex. PPT and B-CD were dissolved in 10 ml of ultra-pure water and stirred for 24h at 37°C. Then the mixture solution was centrifuged (12000 rpm) for 5 min. The supernatant was collected and freeze-dried to obtain the white powdery PPT/B-CD inclusion complex. Rhodamine B/B-CD(R-B/B-CD) inclusion complex was prepared in the same way.

2.6. Water solubility

Excessive PPT, PPT/ β -CD and PPT/B-CD inclusion compound were suspended in 200 μ l of water respectively and the mixture was stirred at 25°C for 24 h. After centrifugation, the supernatant was taken and the absorbance of PPT was measured at 291nm with an UV spectrophotometer.

2.7. Characterization

2.7.1. UV spectroscopy

In order to evaluate the differences of UV-spectra between complexed and uncomplexed PPT, UV-spectra with different concentration of B-CD was recorded by UV Spectrophotometer. Due to the poor solubility of PPT, water/ethanol (V:V=15:1) solution was used in the measurements. Then the concentration of PPT was kept constant while the mass ratio of B-CD/PPT was varied from 0 to 10. The UV-vis spectrum was recorded on UV Spectrophotometer at 200-400nm.

2.7.2. ¹H NMR spectroscopy

All ¹H NMR spectra were recorded with a Bruker AC-400 spectrometer(S-witzerland) in DMSO d₆ (Qiu et al., 2019).

2.7.3. X-ray diffractometry(XRD)

The XRD patterns of PPT, B-CD, PPT/B-CD and physical mixture were obtained by a Philips X'Pert Pro diffractometer, with CuK α radiation, current 40 mA, voltage 40 kV. A scanning speed of 0.15°/min was used at a diffraction angle of 2 θ in the range of 5-60°.

2.7.4. Scanning electron microscopy(SEM)

The surface morphology of the PPT, B-CD, PPT/B-CD and physical mixture was observed by electron microscopy(Jeol,JSM-7500F) on an excitation voltage of 15.0kV.

2.8. In vitro release study

The *in vitro* release of PPT from inclusion complex was determined by membrane diffusion technique (Granero et al., 2008). PPT/B-CD inclusion complex and PPT/ β -CD inclusion complex were dissolved in dialysis bags containing 2ml PBS (pH 7.4) solution, respectively. Dialysis bags were placed in a solution of 200ml PBS(pH 7.4) and shaken at 37°C. At determined time intervals, 2ml of external solution was withdrawn and replaced with an equal volume of fresh PBS solution. The PPT content in the withdrawn medium was determined by the UV/VIS spectroscopy at 291nm. The result was the average of the three runs.

2.9. Cell uptake assay

MDA-M231 cells were cultured in DMEM medium supplemented with 10% heat-inactivated FBS(fetal bovine serum), 1% non-essential amino acid and 100mg/L gentamycin at 37°C in an incubator containing 5% CO₂ (Kiss et al., 2010). The cells were seeded at a density of 2×10^5 cells/well in 6-well plates and incubated overnight (37°C). Then the cells were treated with Rhodamine B (R-B) (5 μ g/ml), R-B/ β -CD and R-B/B-CD (5 μ g/ml). After incubating at 37°C for 0.5h, the cells were rinsed twice with cold PBS, fixed with 4% paraformaldehyde for 10 min. Then the paraformaldehyde was removed and washed with PBS. The fluorescence micrographs was collected by a fluorescence microscope (Olympus,BX51).

2.10. Flow cytometry

The MDA-M231 cells were seeded at a density of 2×10^5 cells/per well in 6-well plates and allowed to adhere and grow. R-B, R-B/ β -CD and R-B/B-CD at a final concentration of (3 μ g/ml) were added into each well in 2.0ml DMEM. After incubation for 0.5h, each well was rinsed twice with PBS and cells were harvested with trypsin. Then the cells were collected by centrifugation and washed twice with PBS. The fluorescence intensity was detected by flow cytometry.

2.11. Cell toxicity assay

The MTT (3-(4,5-dimethylthiazol-2-yl)-2,5-diphenyl tetrazolium bromide) assay was used to evaluate the cell viability of B-CD (Ansteinsson et al., 2013). In brief, MDA-M231 cells were seeded at a density of 5×10^3 cells per well in 96-well plates and incubated for 24h. PPT, PPT/ β -CD and PPT/B-CD were diluted in DMEM medium to various concentrations. Then the cells were treated with PPT, PPT/ β -CD and PPT/B-CD at different concentrations and incubated at 37°C in an incubator containing 5% CO₂. Three replicates were performed for each concentration, and the control group were treated with medium without drug. After 48h of incubation, 20 μ l of MTT solution (5mg/ml) was added into each well and incubated for another 4h at 37°C. The culture medium was removed and then 150 μ l of dimethyl sulfoxide (DMSO) was added into each well to dissolve the formazan precipitate. Then the absorbance at 562nm was recorded using a microplate reader to calculate the cell viability.

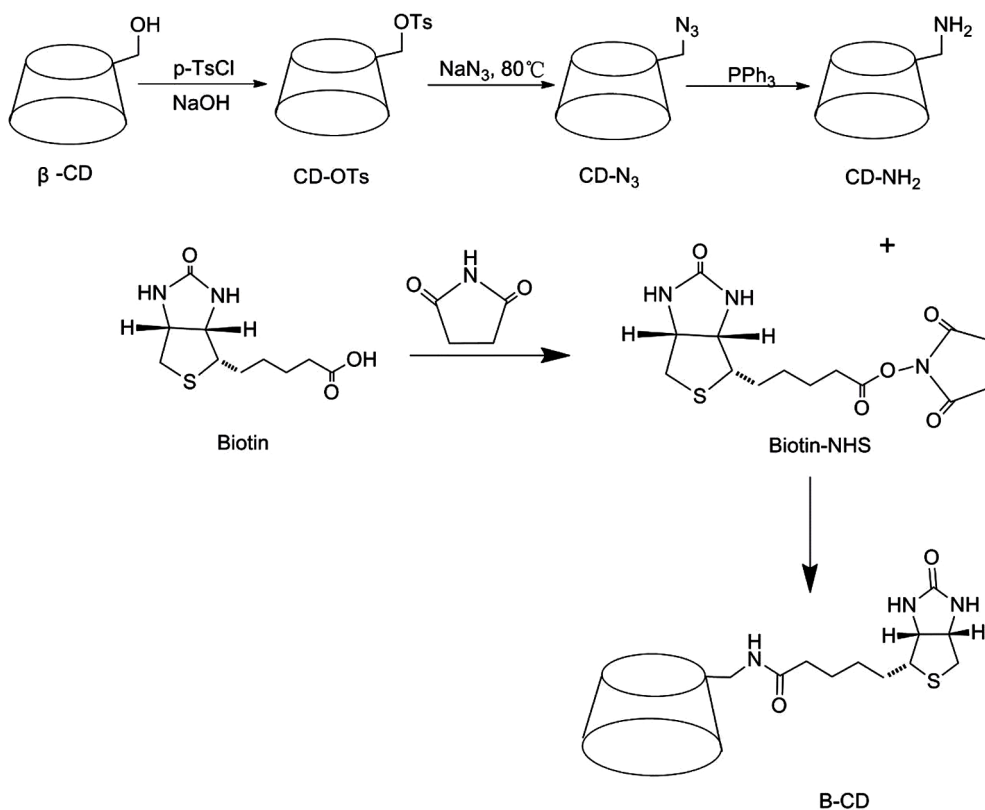


Fig. 1. Synthesis of mono-6-biotin-amino-6-deoxy- β -cyclodextrin(B-CD).

3. Results and Discussion

3.1. Synthesis and water solubility of B-CD

B-CD was successfully synthesized by attachment of biotin with β -CD- NH_2 . β -CD-OTs is the key intermediate for the synthesis of B-CD. Monotosylation of CDs is nonselective and side products such as secondary tosylated derivatives are often produced. Monosulfonation on the primary side with a good yield are preferred to be occurred in basic aqueous medium. Usually, monomodifications of CDs at the 6-position was achieved by reacting with 1 equiv of p -toluenesulfonyl chloride in aqueous alkaline medium. In the present study, regioselective tosylation of a single-OH group at the 6-position was achieved according to the procedure described by Al Temimi et al (Al Temimi et al., 2017). The obtained β -CD-OTs was then reacted with excess sodium azide in hot water to afford β -CD- N_3 in a yield of 88%. Subsequently, β -CD- N_3 was transferred to β -CD- NH_2 through Staudinger Reaction. Next, the carboxyl group of biotin was activated by NHS, and the activated biotin was then coupled with the primary amino group of β -CD- NH_2 leading to the desired product B-CD.

^1H NMR and ^{13}C NMR spectra analysis confirmed the expected structure. We observed some characteristic peaks of β -CD at 5.67-5.73 (m, OH-2, OH-3, 14H), 4.82-4.83(d, H-1, 7H), 4.45-4.48(t, OH-6, 6H), 3.53-3.68(m, H-6, H-5, H-3, 28H) and 3.27-3.37(m, H-2, H-4, 14H) ppm from ^1H NMR spectrum. In addition, we observed that all characteristic peaks of β -CD could be found from the spectra of B-CD. ^1H NMR spectrum and some new characteristic peaks of biotin appeared at 6.35-6.36 (d, 2H), 4.29-4.32(t, 1H), 4.12-4.15(t, 1H), 2.8-2.85(m, 1H) and 1.29-1.63(m, 8H) ppm. NMR results demonstrated that biotin was conjugated at 6-position of β -CD. The number of biotin molecules attached to the β -CD was determined by using the integral unit ratio of the ^1H NMR peak of the B-CD and the DS was calculated to be 15.16%. These results indicated that B-CD was successfully synthesized.

We also used ^{13}C NMR analysis to identify B-CD structure and determine the replacement site. We observed that β -CD had some peaks of different sugar carbons at 102.38(C1), 81.97(C4), 73.5(C2), 72.84 (C3), 72.48(C5) and 60.37(C6) ppm. In addition, we found some new biotin peaks at 162.78-163.21(amides carbon) and 25.63-35.42(methylene carbon) ppm in B-CD. However, after β -CD was modified by biotin, the chemical shift of C6 carbon(55.9 ppm) changed obviously and C2 carbon(73.5 ppm), C3 carbon(72.89 ppm) had very similar chemical shifts in both spectra. The chemical shift changes of ^{13}C NMR demonstrate that biotin modified β -CD occurs at the OH-6 position and these results also support the analyses of ^1H NMR.

Modification of hydroxyl groups could significantly enhance the solubility of β -CD. In the present study, biotin was successfully conjugated with β -CD at the 6-position and the resulting B-CD conjugate displayed a dramatic increase in water solubility. It could be found in Fig. 2a that no white precipitate was observed when the concentration of B-CD increased to 30g/100ml. Only 1.85g of β -CD can be dissolved in 100ml water at 25°C , while more than 30g of B-CD can be dissolved in 100ml water at the same temperature, indicating that B-CD was at least 16 times more soluble than β -CD in water. In addition, the water solubility of B-CD was significantly higher than that of α -CD(14.5g/100ml) and γ -CD(23.2g/100ml) at 25°C (Qiu et al., 2017). This may be because the linking biotin destroys the rigid structure of β -CD and thus increases its water solubility.

3.2. Phase solubility diagram analysis

The phase solubility assay is a useful method to study the inclusion complexation of hydrophobic drugs with CDs in water because it not only provides information on the solubility enhancement of CDs but also inclusion stoichiometry and apparent stability constant (K_s) of the complex (Wang et al., 2007). The phase solubility diagrams of PPT and B-CD were shown in Fig. 2b. It can be seen that the aqueous solubility of

PPT increased linearly with increasing of B-CD concentration in the range of 0 to 10 mM. The correlation coefficient (R^2) of the phase solubility diagram was found to be 0.9927 ($R^2 > 0.9900$), so the phase solubility diagram was considered to be a straight line and can be regarded as A_L type (Waleczek et al., 2003). Because the slope of the phase solubility curve was found to be less than 1, it could be suggested that the formation of PPT/B-CD complex was first order complex with respect of B-CD concentration (Fernandes et al., 2002). The stability constants of PPT/B-CD complexes were calculated by using the following equation:

$$K_s = \text{slope}/S_0(1-\text{slope}) \quad (1)$$

where S_0 is the intrinsic PPT solubility when no B-CD is present in the solution and slope is value obtained from the straight line of the phase solubility diagram. K_s value is frequently reported between 50 and 2000M^{-1} (Hu et al., 2012). The K_s value was calculated to be 415.29M^{-1} in our study, suggested a favorable inclusion complex of PPT/B-CD was formed. However, it was found that PPT/ β -CD inclusion compound has very low stability constant ($K_s=128\text{M}^{-1}$) in aqueous solution (Ma et al., 2000). In our study, the stability constant of PPT/B-CD inclusion compound was approximately 3.2 times that of PPT/ β -CD inclusion compound, so we can infer that B-CD complexed drugs are more stable than β -CD complexed drugs. The water solubility of PPT was 0.37mM and was found to increase to 1.76mM in the presence of 10mM B-CD. Clearly, the inclusion complex of PPT/B-CD was formed and the resulting complex can increase the aqueous solubility of PPT.

It can be seen from equation 1 that S_0 has strong influence on K_s values. Previous reports have shown that S_0 was strongly affected by pharmaceutical excipients and complexation. Therefore, the stability constants (K_s) are often inaccurate and get easily affected by the composition of the aqueous complexation medium (Loftsson et al., 2007). Thus, a more accurate method for calculation of the complexation efficiency (CE) was proposed by Loftsson (Loftsson et al., 1999; Loftsson and Brewster, 2012). The CE value of the complex of PPT/B-CD was calculated by using the following equation:

$$\text{CE} = \text{slope}/(1-\text{slope}) \quad (2)$$

where slope was the slope obtained in phase solubility diagram. CE is more reliable because the CE value is only determined by the slope of the phase solubility profile. In our study, the CE value was calculated to be 0.162 according to the phase solubility diagram. CE is also defined as the concentration ratio of CD in complex to free CD (Loftsson et al., 2005). Therefore, the concentration ratio between PPT and B-CD molecules can be calculated to be 1:7 from CE according to equation 3. The concentration ratio between drug and CD indicated that on an average about 1 out every 7 B-CD molecules are forming aqueous soluble inclusion complex with PPT.

$$\text{Drug:CD} = 1:[(\text{CE}+1)/\text{CE}] \quad (3)$$

The stoichiometry of the inclusion complex between PPT and B-CD was also studied by Job's plot. The job's plot method has long been utilized to evaluate the stoichiometric ratio of two interacting chemical entities. In this method, the total molar concentration of PPT and B-CD is held constant while the molar fraction of host: guest varied continuously. The absorbance is recorded and plotted against the mole fractions of the complexing components to give the Jobs' curve. The complexation stoichiometry is then obtained from the ratio of the mole fraction observed at the maximum of the curve (Huang et al., 2003). As shown in Fig. 2c, the maximum peak was found at a molar fraction of about 0.5, suggesting that the stoichiometric ratio of PPT/B-CD complex was 1:1, which was in accordance with the phase solubility study.

3.3. Preparation of PPT/B-CD inclusion complex

Various methods such as solvent evaporation, freeze-drying,

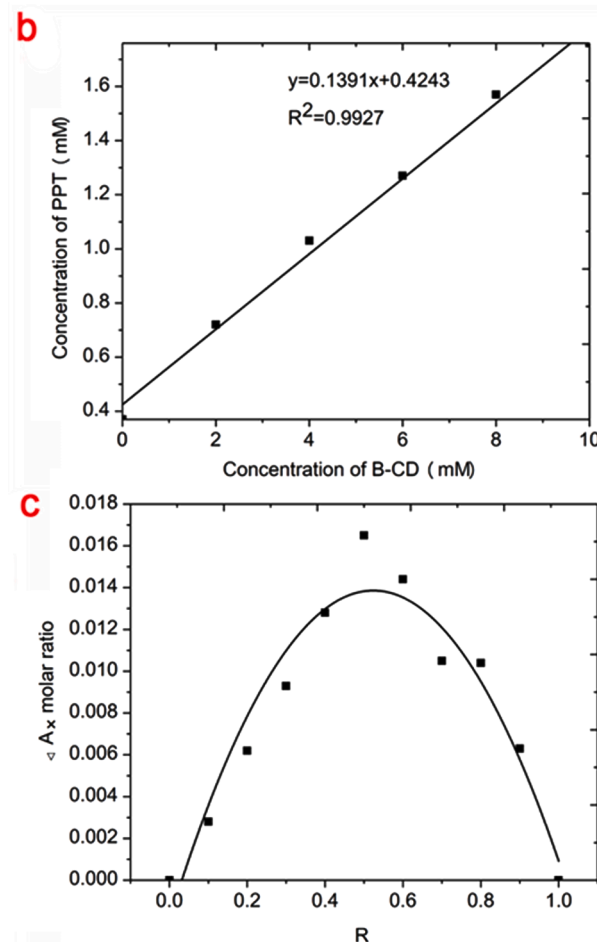
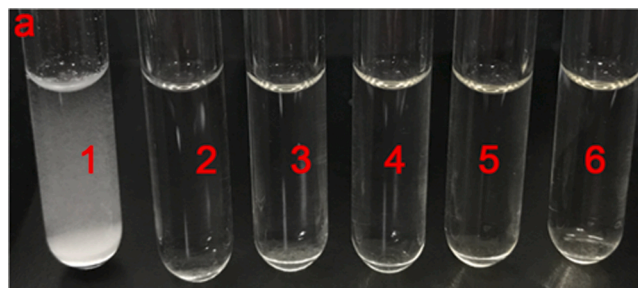


Fig. 2. (a) Solubility of β -CD and B-CD (1: β -CD, 7.5g/100 ml; 2: B-CD, 7.5g/100ml; 3: B-CD, 12.5g/100ml; 4: B-CD, 17.5g/100 ml; 5: B-CD, 25g/100ml; 6: B-CD, 30g/100 ml); (b) Phase solubility diagram of PPT/B-CD complex system at 37°C . The concentration of B-CD was in the range of 0-10mM; (c) Job's plot for different molar fraction of PPT and B-CD.

kneading, spray drying and coprecipitation have been reported for inclusion complex preparation. In our study, PPT/B-CD inclusion complexes were prepared by co-evaporation and freeze-drying method. Evaporation method was first chosen to prepare the inclusion complex of PPT/B-CD. However, we found that B-CD was poorly soluble in ethanol, thus, evaporation method was not suitable for the preparation of PPT/B-CD. Freeze-drying method was chosen and the mass ratio between B-CD and PPT was optimized. The optimal mass ratio of B-CD to PPT for the freeze-drying method was found to be 1:21. In the above phase solubility study, we calculated from CE that the concentration molar ratio of PPT to B-CD was 1:7. The molecule weight of PPT is 414Da and B-CD is 1360Da. Therefore, we can calculate that corresponding optimal molar ratio of PPT:B-CD for the preparation of PPT/B-

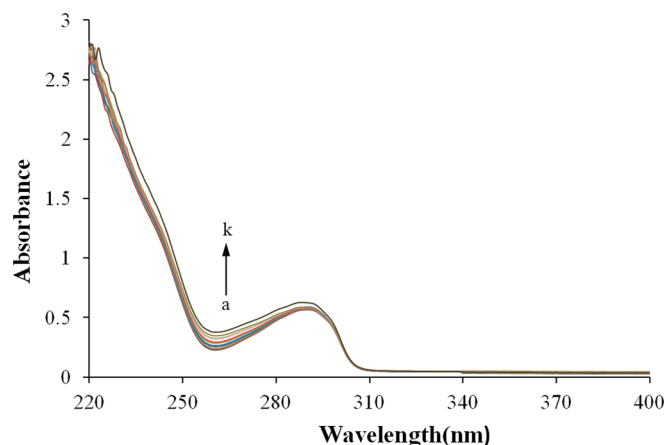


Fig. 3. The effect of B-CD concentration on the UV-vis spectra of PPT(50µg/ml). The B-CD concentration was (a) 0µg/ml; (b) 50µg/ml; (c) 100µg/ml; (d) 150µg/ml; (e) 200µg/ml; (f) 250µg/ml; (g) 300µg/ml; (h) 350µg/ml; (i) 400µg/ml; (j) 450µg/ml; (k) 500µg/ml, respectively.

CD inclusion complex was 1:7, which was coincidence with the phase solubility study.

3.4. Water solubility of PPT/B-CD complexes

The water solubility of PPT, PPT/ β -CD and PPT/B-CD complexes were evaluated by the preparation of saturated solution. The results showed that the solubility of PPT in water was increased to 843.31µg/ml and 2424.42 µg/ml(25°C) by complexation with β -CD and B-CD compared with natural PPT(278.2 µg/ml), respectively. Although both β -CD and B-CD have solubilization effect on PPT, the solubilization effect of B-CD is obviously stronger. And we found that the solubility of PPT/B-CD complexes were 9 times more soluble than PPT. The solubility of PPT/B-CD complexes were 3 times more soluble than PPT/ β -CD. These results indicated that the PPT complexed with B-CD can improve the solubility of the PPT, which is beneficial to the utilization of the compound as a medical product.

3.5. Characterization

3.5.1. UV spectroscopy

Ultraviolet spectrophotometry is the most commonly used characterization technique to investigate the influence of CDs on the absorption of guest molecules(Raza et al., 2017). The complex formation between PPT and B-CD was studied by spectral shift method. The changes in ultraviolet absorption of PPT in aqueous solution before and after B-CD added were shown in the Fig. 3. In the absence of B-CD, a typical absorption peak of PPT was observed at 291nm (Fig. 3). The UV absorption spectrum of PPT/B-CD was very similar to that of PPT. It was worth noting that the absorbance strength of PPT at 291nm gradually increased with the increase of B-CD/PPT mass ratio from 1 to 10. With the increase of B-CD concentration, a slight blue shift of the absorption peak was observed in PPT/B-CD complex curve. These results may possibility indicate the formation of the inclusion complex between PPT and B-CD.

3.5.2. ^1H NMR spectroscopy analysis

The formation of inclusion complexes could be evaluated by ^1H NMR due to chemical shift changes were observed in both host and guest molecules (Liu et al., 2014). The ^1H NMR spectrums of B-CD, PPT and PPT/B-CD inclusion complex were shown in Fig. 4. As can be seen in Fig. 4b, chemical shifts of B-CD were observed at δ 1.0-6.70 ppm. Meanwhile, chemical shifts of PPT were observed at δ 2.0-7.20 ppm in

the Fig. 4a. In addition, we can find that the chemical shifts of PPT protons in the spectrum of the inclusion complex appeared at δ 3.47-7.20 ppm (Fig. 4c). The result confirmed the presence of PPT in the inclusion complex.

As shown in the Table 1, in order to further explore the formation of inclusion complex, the chemical shifts of B-CD and PPT/B-CD complex were studied. After complexation with PPT, the H-3 proton of B-CD shifted -0.021ppm, the H-6 proton of B-CD shifted -0.023 ppm. Since H-3 proton is located in the interior of B-CD, the relatively high displacement of the H-3 proton indicated that part of the PPT was encaged in the B-CD cavity to form inclusion complexes. For H-3 proton is located on the inner surface of B-CD cavity and populated in the wide side (Yang et al., 2009), we can deduce that PPT could be encaged into the B-CD cavity from the wide side. To further explore the interactions between PPT and B-CD, chemical shift changes of PPT were also listed in table 1. After complexation with B-CD, most significant shift changes were observed in H-2', H-5', H-2, H-6 and H-10 protons, which attributed to A, B and E ring of PPT. Based on these results, we can infer that the A and B ring of PPT penetrated into B-CD from the wide side with A ring deeply inserted into the cavity.

Nuclear Overhauser effect (NOE) cross-correlation in 2D NMR spectroscopy provides powerful evidence about the spatial proximity between host and guest molecules (Xu et al., 2017). In order to obtain more information about the correlation between PPT and B-CD, ROESY spectrum of the PPT/B-CD complex was recorded and shown in Fig. 5a. The ROESY spectrum presented a significant cross-peaks between OH-3 and H-2' of B-CD, and H-7', H-7 and/or OH-7' of PPT, indicated that part of the ring of PPT was encaged in the B-CD cavity and the C ring of PPT was located on the wide edge. From the chemical structure of PPT, we can see an aromatic ring (E) with three methoxy groups and a hydroxy group are located on C ring, consequently, C ring is larger than A, B and D ring and difficult to be encapsulated by B-CD cavity. Based on these results together with the ^1H NMR results, we can infer that A ring and B ring of PPT entered into the B-CD cavity from the wide side with C ring located on the edge of the wide side and the possible inclusion mode for the PPT/B-CD complex was presented in Fig. 5b.

3.5.3. PXRD analysis

The inclusion complex of PPT/B-CD was further confirmed by XRD. The XRD patterns of PPT, B-CD, PPT/B-CD and physical mixture were presented in Fig. 6. As shown in Fig. 6a, the XRD spectrogram of PPT exhibited a series of sharp diffraction peaks, suggesting crystalline nature of the PPT. In contrast, no crystalline peak was observed in the spectrogram of B-CD (Fig. 6b), indicating its amorphous nature. The peaks corresponding to PPT have been observed in the physical mixture (Fig. 6d), but with less intensity. These results showed that the crystalline nature of the PPT remained unchanged in the physical mixture. As illustrated in Fig. 6c, no sharp peaks were observed in the XRD spectrogram of PPT/B-CD inclusion complex, indicating the crystalline nature of PPT had disappeared in the inclusion complex. The lack of crystallinity provided evidence for the formation of an inclusion complex (Williams et al., 1998). This phenomenon indicated that there was an interaction between PPT and B-CD, which may probably be the consequence of the formation of a new complex.

3.5.4. SEM analysis

SEM images were obtained to visualize the microstructure and surface morphology changes of the host-guest complexes (Tang et al., 2015). The scanning electron microphotographs of PPT, B-CD, inclusion complex and their physical mixture were shown in Fig. 7. The microphotograph of PPT (Fig. 7a) appeared as irregular and three-dimensional crystal (Sinha et al., 2005). As shown in the Fig. 7b, the B-CD was observed to be an irregular parallelogram shape. Both PPT and B-CD structure could be observed in the physical mixture (Fig. 7d), suggesting that there is no interaction between PPT and B-CD in the solid state. PPT/B-CD complex showed a typical morphology of inclusion

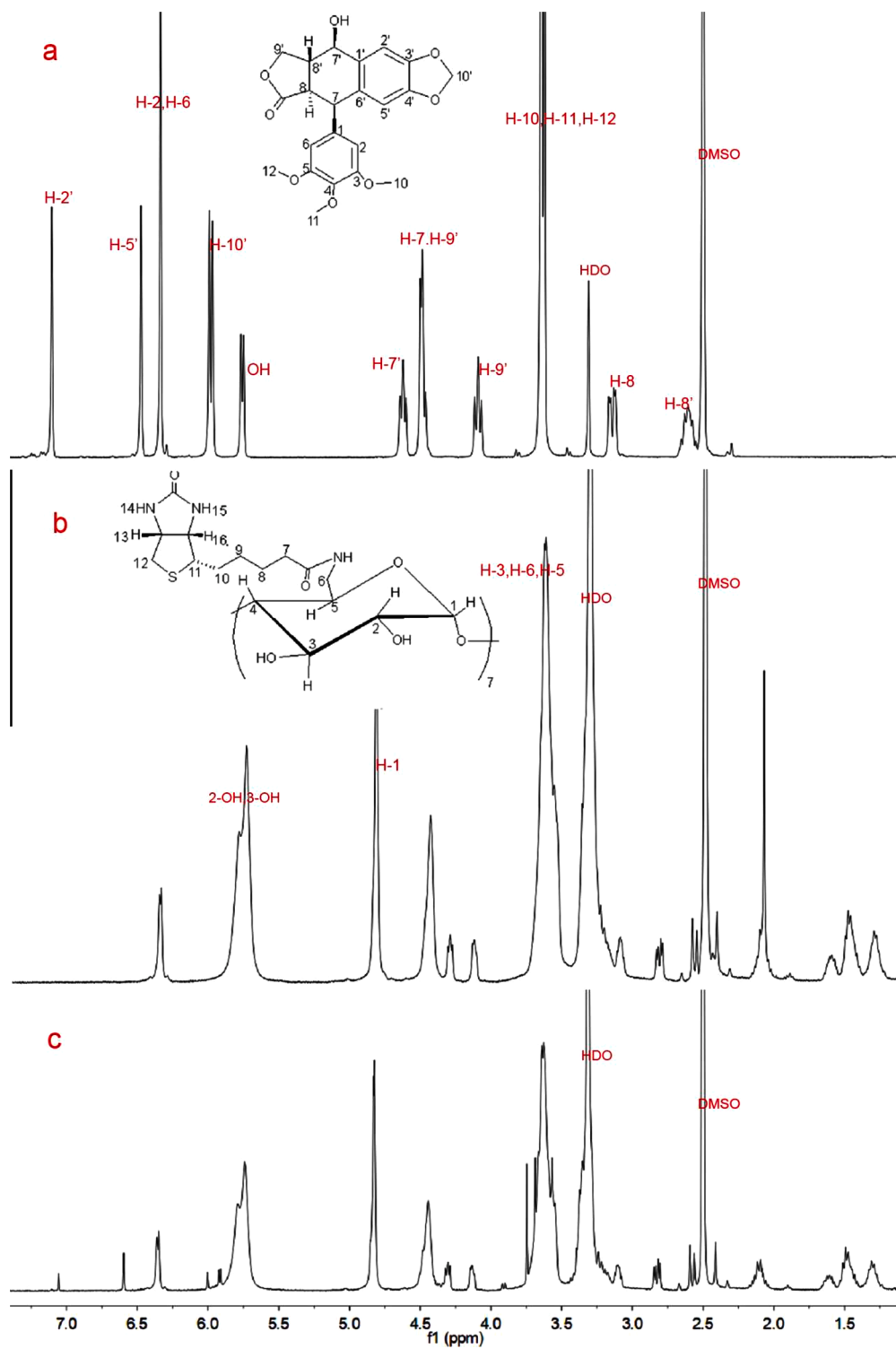


Fig. 4. ^1H NMR spectra of (a) PPT; (b) B-CD; (c) PPT/B-CD complex in DMSO-d_6 .

Table 1

Variation of ^1H NMR chemical shifts (δ/ppm) of B-CD, PPT and PPT/B-CD inclusion complex.

Protons	B-CD	Complex	$\Delta\delta_1(\text{ppm})$
H ₁	4.820	4.817	0.003±0.001
H ₂	overlap with HDO	overlap with HDO	—
H ₃	3.670	3.691	-0.021±0.003
H ₄	overlap with HDO	overlap with HDO	—
H ₅	3.568	3.565	0.003±0.002
2-OH	5.793	5.793	0
3-OH	5.750	5.745	0.005±0.001
H ₆	3.651	3.674	-0.023±0.005
6-OH	4.449	4.439	0.010±0.004
PPT		Complex	$\Delta\delta_1(\text{ppm})$
2'-H	7.106	7.071	0.035±0.012
5'-H	6.474	6.554	-0.080±0.033
2-H	6.336	6.361	-0.025±0.000
6-H	6.331	6.342	-0.011±0.004
10'-H	5.992	5.999	-0.007±0.003

complex in Fig. 7c with amorphous sheet structure of very homogeneous (Bhargava and Agrawal, 2008; Corti et al., 2007). In addition, the morphology of PPT and B-CD completely disappeared in the resulting inclusion complex. SEM analysis also suggest that the PPT/B-CD inclusion complex was amorphous since no crystals were seen. These results indicated the formation of a new solid phase.

3.6. In vitro release study

The mean cumulative release of PPT from free PPT/ β -CD and PPT/B-CD inclusion complex in PBS was shown in Fig. 8. Both formulations had burst release. Almost 75% and 70% of drug were released from PPT/ β -CD and PPT/B-CD complex in the first 2h, about 94% of drug was released from PPT/ β -CD complex in the first 3h, while about 83% was released at the same time. It can be observed that the rate of drug release from PPT/B-CD inclusion complex was slightly slower than from PPT/ β -CD. Since a higher K_s value of PPT/B-CD was obtained in comparison with PPT/ β -CD in phase solubility study. The relatively slower release of PPT/B-CD might be due to a more stable inclusion complex formed between PPT and B-CD compared with PPT and β -CD.

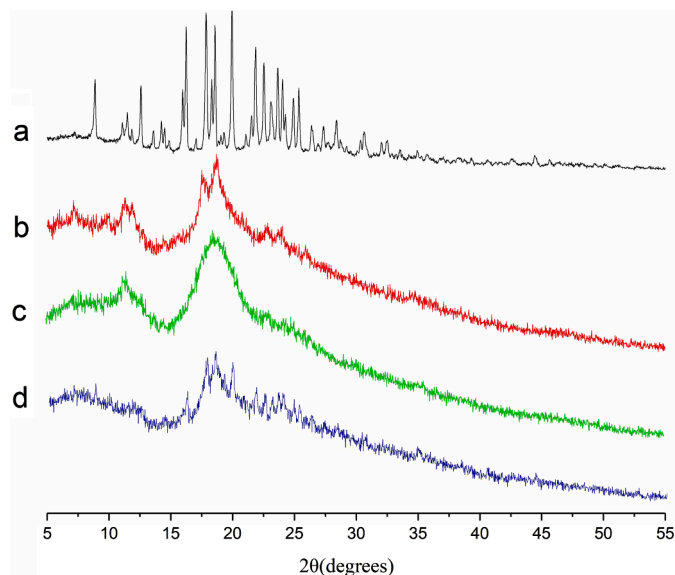


Fig. 6. Powder X-ray diffraction patterns of (a) pure podophyllotoxin; (b) B-CD; (c) PPT/B-CD complex; (d) PPT and B-CD physical mixture.

3.7. Cell uptake and cytotoxicity

Rhodamine B was applied to monitor their uptake in MDA-M231 cells (Han et al., 2018). Cellular uptake of rhodamine B labeled with free rhodamine B, R-B/ β -CD inclusion complex and R-B/ β -CD inclusion complex was analyzed by fluorescence microscopy. Fig. 9 showed the cellular uptake of rhodamine B from free rhodamine B solution (Fig. 9c), R-B/ β -CD inclusion complex (Fig. 9b) and R-B/B-CD inclusion complex (Fig. 9a) in MDA-M231 cells for 0.5 h. We can observe that the fluorescence intensity of R-B/B-CD is the strongest in comparison with R-B and R-B/ β -CD, which proves that an enhanced cellular uptake of R-B for the R-B/B-CD inclusion complex. In addition, we also observed that the fluorescence intensity of R-B/B-CD was the highest in the flow diagram (Fig. 9d) at the same time, which was consistent with the results of cell uptake fluorescence diagram. Therefore, combining the results of fluorescence and flow cytometry, we can infer that B-CD enhanced the

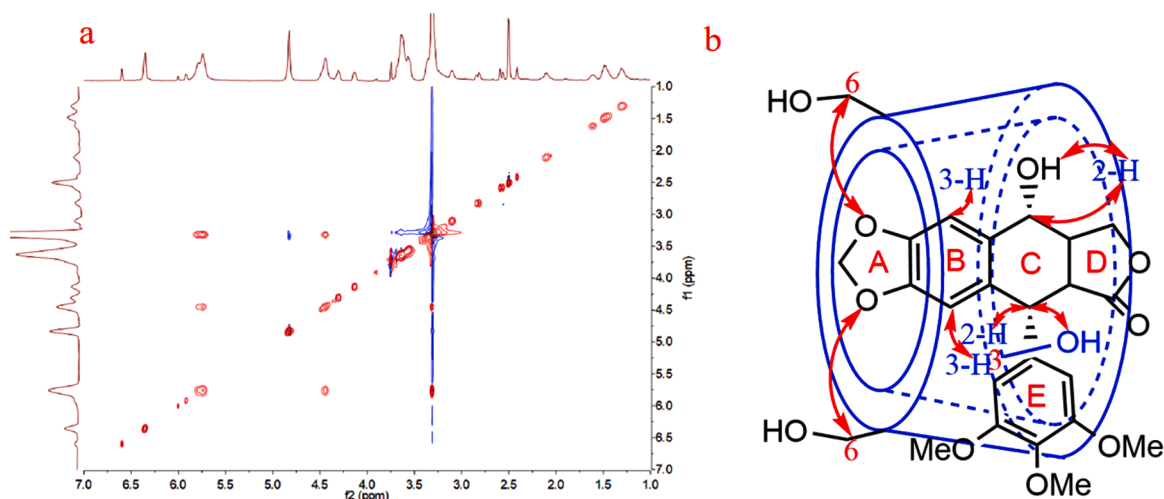


Fig. 5. (a) ROESY spectrum of PPT/B-CD complex; (b) Possible inclusion mode of PPT/B-CD inclusion complex.

drug uptake possibly due to the aid of biotin receptor mediated endocytosis.

In vitro cytotoxicity of the PPT, PPT/ β -CD inclusion complex and PPT/B-CD inclusion complex was evaluated against MDA-M231 cells. Fig. 9e showed the cytotoxicity of free PPT, PPT/ β -CD and PPT/B-CD solution over several time points at the same concentration (81 μ M). PPT/B-CD inclusion complex showed the least cell viability. Furthermore, the IC₅₀ of PPT/B-CD was about 8 times lower than that of PPT/ β -CD and 14 times lower than that of PPT for 72 h, indicating that PPT/B-CD had the greatest inhibitory effect on MDA-M231 cells compared to PPT/ β -CD and PPT (Table 2). These results demonstrated that PPT/B-CD enhanced the cytotoxicity of PPT and PPT/ β -CD probably due to biotin-mediated cell uptake and enhanced water solubility of PPT.

4. Conclusions

In this study, a mono-6-biotin-amino-6-deoxy- β -cyclodextrin conjugate was successfully synthesized and the resulting conjugate notably improved the water solubility of β -cyclodextrin. Based on this conjugate, podophyllotoxin/ mono-6-biotin-amino-6-deoxy- β -cyclodextrin complex was prepared by freeze-drying method. The solubility of podophyllotoxin was greatly improved after being complexed with mono-6-biotin-amino-6-deoxy- β -cyclodextrin. The phase solubility study demonstrated that podophyllotoxin/mo-6-biotin-amino-6-deoxy-

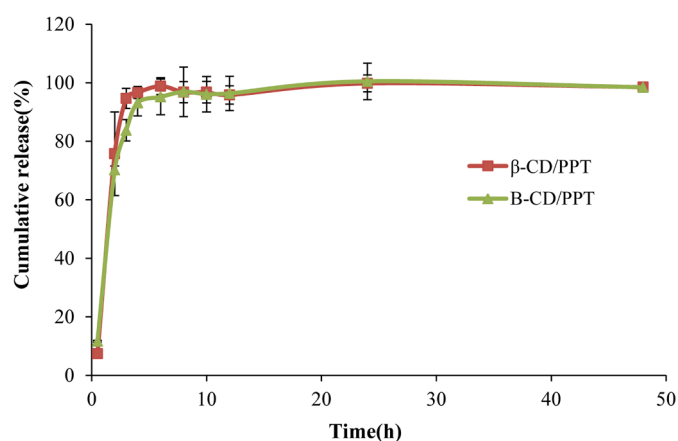


Fig. 8. *In vitro* release profiles of PPT/B-CD complex and PPT/ β -CD complex using dialysis bag technique in PBS (7.4).

β -cyclodextrin complex was more stable than podophyllotoxin/ β -cyclodextrin complex. Powder X-ray diffraction and Scanning electron microscopy demonstrated the formation of podophyllotoxin/mo-6-

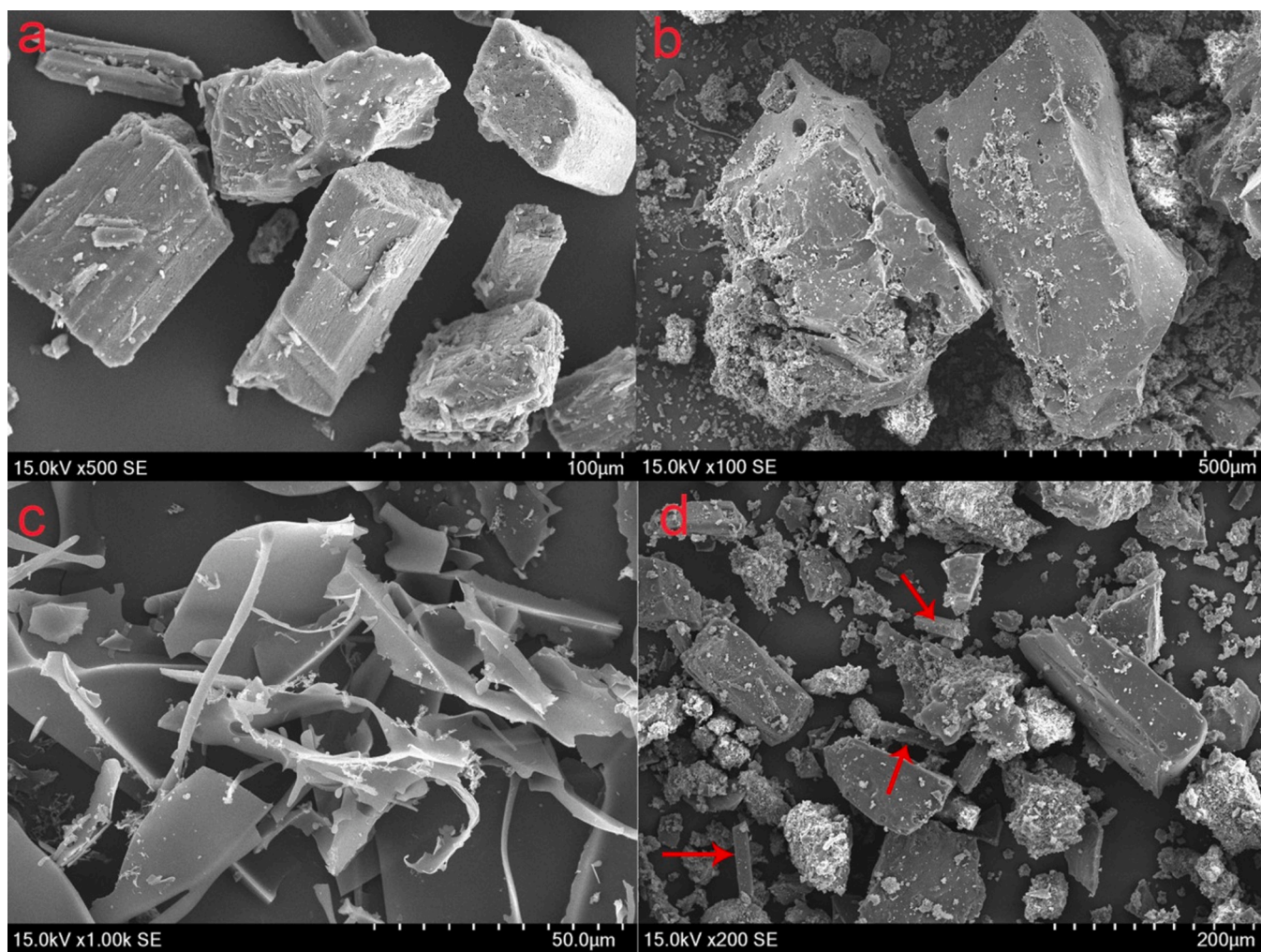


Fig. 7. Scanning electron microphotographs: (a) pure podophyllotoxin; (b) B-CD; (c) PPT/B-CD complex; (d) podophyllotoxin and B-CD physical mixture.

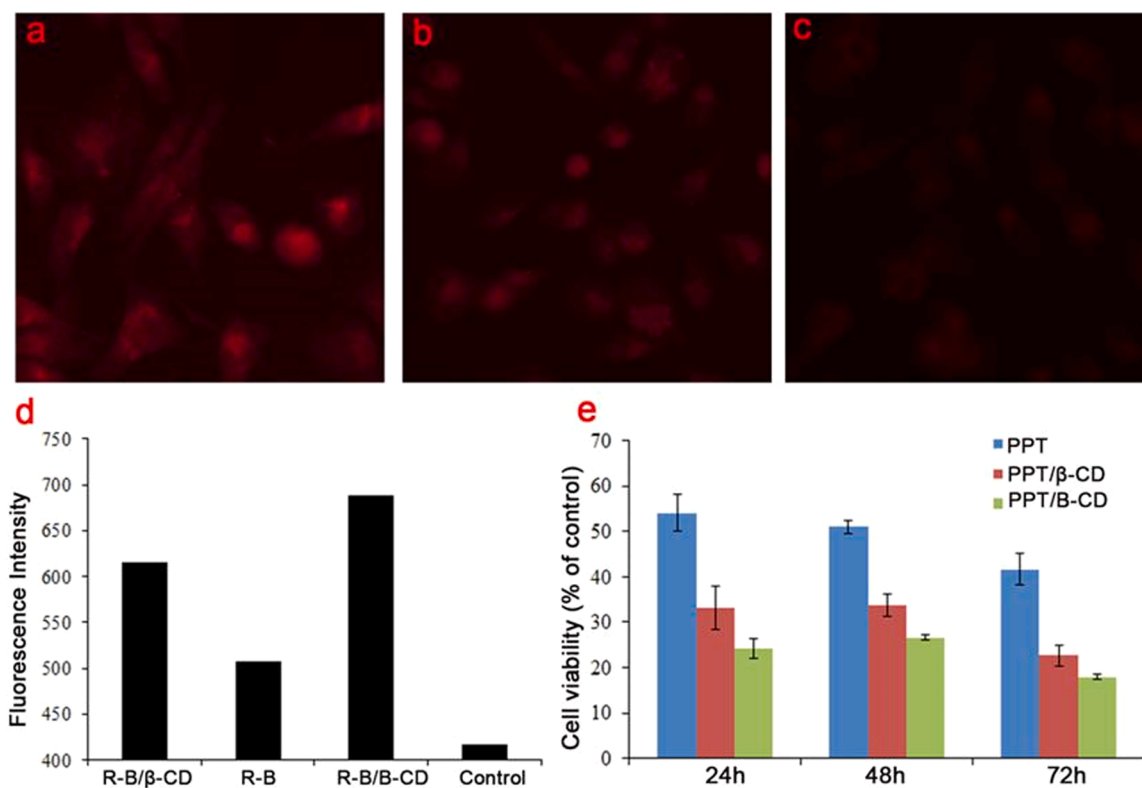


Fig. 9. Fluorescence images of R-B/B-CD(a), R-B/β-CD (b) and R-B(c) in MDA-M231 cells; (d) Flow cytometric analysis of the cellular uptake of PPT/B-CD complex in MDA-M231 cells after 0.5 h incubation; (e) *In vitro* cytotoxicity of PPT/B-CD complex against MDA-M231 cells.

Table 2

Cytotoxicities (IC₅₀) of PPT, PPT/β-CD inclusion complex and PPT/B-CD inclusion complex against MDA-M231 cell lines.

Time	PPT/B-CD (μM)	PPT/β-CD (μM)	PPT(μM)
24h	26.57	>81	>81
48h	14.51±2.16	19.65±3.26	66.31±1.51
72h	1.85±0.98	14.5±3.14	25.38±4.62

biotin-amino-6-deoxy-β-cyclodextrin inclusion complex. The possible inclusion mode of podophyllotoxin/mono-6-biotin-amino-6-deoxy-β-cyclodextrin complex was inferred from the Proton Nuclear Magnetic Resonance and Rotating-frame Overhauser Effect Spectroscopy. Moreover, the cell uptake study showed that the introduction of biotin increased the cellular uptake of rhodamine-B/mono-6-biotin-amino-6-deoxy-β-cyclodextrin complex. Podophyllotoxin/mono-6-biotin-amino-6-deoxy-β-cyclodextrin demonstrated superior antitumor activity as compared with podophyllotoxin and podophyllotoxin/β-cyclodextrin in breast cancer. It may be concluded that the introduction of biotin enhanced the selectivity of podophyllotoxin complex towards tumor cells. Therefore, the biotin conjugated β-cyclodextrin based inclusion complex might be used as a potential anticancer drug carrier for the treatment of cancer.

Credit Author Statement

Xiu Zhao: Investigation, Methodology, Formal analysis, Validation, Writing - Original Draft;

Neng Qiu: Conceptualization, Methodology, Resources, Writing-Review & Editing, Investigation, Supervision, Funding acquisition;

Yingyu Ma: Investigation;

Junda Liu: Methodology;

Lianying An: Resources;

Teng Zhang: Investigation;

Ziqin Li: Investigation;

Xu Han: Investigation;

Lijuan Chen: Review & Editing.

Acknowledgements

This research was supported by the grant of National Natural Science Foundation of China (NSFC) (No. 21606025), the Foundation for the Youth Scholars of Chengdu University of Technology, China (No.10912-KYGG2019-04282) and National Training Program of Innovation and Entrepreneurship for Undergraduates (30800-2019DCXM006).

References

- Stappaerts, J., Berben, P., Cevik, I., Augustijns, P., 2018. The effect of 2-hydroxypropyl-β-cyclodextrin on the intestinal permeation through mucus. *Eur. J. Pharm. Sci.* 114, 238–244. <https://doi.org/10.1016/j.ejps.2017.12.014> <https://doi.org/>
- Anil Kumar, K., Kumar Singh, S., Siva Kumar, B., Mukesh, D., 2007. Synthesis, antifungal activity evaluation and QSAR studies on podophyllotoxin derivatives. *Open Chem* 5, 880–897.
- Anstinson, V., Kopperud, H.B., Morisbak, E., Samuelsen, J.T., 2013. Cell toxicity of methacrylate monomers-The role of glutathione adduct formation. *J. Biomed. Mater. Res., Part A* 101 (12), 3504–3510 <https://doi.org/10.1002/jbm.a.34652>
- Al Temimi, H.K., Boltje, T.J., Daniel, Z., Rutjes, F.P.J.T., Feiters, M.C., 2017. Peptide-Appended Permethylated β-Cyclodextrins with Hydrophilic and Hydrophobic Spacers. *Bioconjug. Chem* 28 (8), 2160–2166. <https://doi.org/10.1021/acs.bioconjchem.7b00319> <https://doi.org/>
- Abbas, H.K., Al, T., Boltje, T.J., Daniel, Z., Rutjes, F., Feiters, M., 2017. Peptide-Appended Permethylated β-Cyclodextrins with Hydrophilic and Hydrophobic Spacers. *Bioconjug. Chem.* 28, 2160–2166. <https://doi.org/10.1021/acs.bioconjchem.7b00319> <https://doi.org/>
- Bhargava, S., Agrawal, G.P., 2008. Preparation & Characterization of Solid Inclusion Complex of Cefpodoxime Proxetil with β-Cyclodextrin. *Curr. Drug Delivery* 5, 1–6. <https://doi.org/10.2174/156720108783330998> <https://doi.org/>
- Bian, Q.Q., Xiao, Y., Lang, M.D., 2012. Thermoresponsive biotinylated star amphiphilic block copolymer: Synthesis, self-assembly, and specific target recognition. *Polymer* 53, 1684–1693. <https://doi.org/10.1016/j.polymer.2012.02.031> <https://doi.org/>
- Bagheri, M., Shateri, S., Niknejad, H., Entezami, A.A., 2014. Thermosensitive biotinylated hydroxypropyl cellulose-based polymer micelles as a nanocarrier for

- cancer-targeted drug delivery. *J. Poly. Res.* 21, 567. <https://doi.org/10.1007/s10965-014-0567-4> <https://doi.org/>.
- Carmen, G., Miguel, S., Inigo, X., Garcia, Z., Itziar, V., Cristina, M.O., Carmen, M., Arantza, Z., 2005. HPLC and solubility study of the interaction between pindolol and cyclodextrins. *J. Pharm. Biomed. Anal.* 37, 487–492. <https://doi.org/10.1016/j.jpba.2004.11.008> <https://doi.org/>.
- Corti, G., Capasso, G., Maestrelli, F., Cirri, M., Mura, P., 2007. Physical-chemical characterization of binary systems of metformin hydrochloride with triacetyl- β -cyclodextrin. *J. Pharm. Biomed. Anal.* 45, 480–486. <https://doi.org/10.1016/j.jpba.2007.07.018> <https://doi.org/>.
- Fernandes, C.M., Vieira, M.T., Veiga, F.J.B., 2002. Physicochemical characterization and in vitro dissolution behavior of nicardipine-cyclodextrins inclusion compounds. *Eur. J. Pharm. Sci.* 15, 79–88. [https://doi.org/10.1016/S0928-0987\(01\)00208-1](https://doi.org/10.1016/S0928-0987(01)00208-1) <https://doi.org/>.
- Gordaliza, M., Castro, M.A., Corral, J.M., Feliciano, A.S., 2000. Antitumor properties of podophyllotoxin and related compounds. *Curr. Pharmaceut. Des.* 6, 1811–1839. <https://doi.org/10.2174/1381612003398582> <https://doi.org/>.
- Giri, A., Narasu, M.L., 2000. Production of podophyllotoxin from *Podophyllum hexandrum*: a potential natural product for clinically useful anticancer drugs. *Cytotechnology* 34 (1–2), 17–26. <https://doi.org/10.1023/A:1008138230896> <https://doi.org/>.
- Gould, S., Scott, R.C., 2005. 2-Hydroxypropyl- β -cyclodextrin(H- β -CD): A toxicology review. *Food. Chem. Toxicol.* 43, 1451–1459. <https://doi.org/10.1016/j.fct.2005.03.007> <https://doi.org/>.
- Granero, G.E., Maitre, M.M., Garner, C., Longhi, M.R., 2008. Synthesis, characterization and in vitro release studies of a new acetazolamide-HP- β -CD-TEA inclusion complex. *Eur. J. of Med Chem* 43, 464–470. <https://doi.org/10.1016/j.ejmech.2007.03.037>.
- Gong, N.B., Yang, D.Z., Jin, G.M., Liu, S.C., Du, G.H., Lu, Y., 2019. Structure, characterization, solubility and stability of podophyllotoxin polymorphs. *J. Mol. Struct.* 1195, 323–330. <https://doi.org/10.1016/j.molstruc.2019.05.048> <https://doi.org/>.
- Huang, C.Y., Zhou, R.X., Yang, D.C.H., Chock, P.B., 2003. Application of the continuous variation method to cooperative interactions: mechanism of Fe (II)-ferrozine chelation and conditions leading to anomalous binding. *Bio. Chem* 100, 143–149. [https://doi.org/10.1016/S0301-4622\(02\)00275-2](https://doi.org/10.1016/S0301-4622(02)00275-2) <https://doi.org/>.
- Hu, L.D., Zhang, H.L., Song, W.H., Gu, D.L., Hu, Q.F., 2012. Investigation of inclusion complex of cilindipine with hydroxypropyl- β -cyclodextrin. *Car. Polymers* 90, 1719–1724. <https://doi.org/10.1016/j.carbpol.2012.07.057> <https://doi.org/>.
- Han, S.M., Beak, J.S., Kim, M.S., Hwang, S.J., Cho, C.W., 2018. Surface modification of paclitaxel-loaded liposomes using d- α -tocopheryl polyethylene glycol 1000 succinate: Enhanced cellular uptake and cytotoxicity in multidrug resistant breast cancer cells. *Chem. Phys. Lipids* 213, 39–47. <https://doi.org/10.1016/j.chemphyslip.2018.03.005> <https://doi.org/>.
- Hädärugä, N.G., Bandur, G.N., David, I., Hädärugä, D.I., 2019. A review on thermal analyses of cyclodextrins and cyclodextrin complexes. *Environ. Chem. Lett* 17, 349–373. <https://doi.org/10.1007/s10311-018-0806-8> <https://doi.org/>.
- Imbert, T.F., 1998. Discovery of podophyllotoxins. *Biochimie* 80, 207–222. [https://doi.org/10.1016/S0300-9084\(98\)80004-7](https://doi.org/10.1016/S0300-9084(98)80004-7) <https://doi.org/>.
- Kiss, T., Fenyvesi, F., Bácskay, I., Váradi, J., Fenyvesi, É., Iványi, R., Szente, L., Tóskai, Á., Vecsernyés, M., 2010. Evaluation of the cytotoxicity of β -cyclodextrin derivatives: Evidence for the role of cholesterol extraction. *Eur. J. Pharm. Sci.* 40, 376–380. <https://doi.org/10.1016/j.ejps.2010.04.014> <https://doi.org/>.
- Loftsson, T., Másson, M., Sigurjónsdóttir, J.F., 1999. Methods to enhance the complexation efficiency of cyclodextrins. *STP Pharma Science* 9, 237–242. <https://doi.org/10.1016/j.enganabound.2019.03.028>.
- Liu, X., Lin, H.S., Thenmozhiyal, J.C., Chan, S.Y., HO, P.C., 2003. Inclusion of Acitretin into Cyclodextrins: Phase Solubility, Photostability, and Physicochemical Characterization. *J. Pharm. Sci.* 92, 2449–2457. <https://doi.org/10.1002/jps.10495> <https://doi.org/>.
- Loftsson, T., Hreinsdóttir, D., Másson, M., 2005. Evaluation of cyclodextrin solubilization of drugs. *Int. J. Pharm* 302, 18–28. <https://doi.org/10.1016/j.ijpharm.2005.05.042> <https://doi.org/>.
- Loftsson, T., Hreinsdóttir, D., Másson, M., 2007. The complexation efficiency. *J. Inclusion Phenom. Macrocyclic Chem* 57, 545–552. <https://doi.org/10.1007/s10847-006-9247-2> <https://doi.org/>.
- Lammers, T., Hennink, W.E., Storm, G., 2008. Tumour-targeted nanomedicines: principles and practice. *Br. J. Cancer* 99, 392–397. <https://doi.org/10.1038/sj.bjc.6604483> <https://doi.org/>.
- Loftsson, T., Brewster, M.E., 2012. Cyclodextrins as functional excipients: methods to enhance complexation efficiency. *J. Pharm. Sci.* 101, 3019–3032. <https://doi.org/10.1002/jps.23077> <https://doi.org/>.
- Liu, M.N., Cao, W., Sun, Y.H., He, Z.G., 2014. Preparation, characterization and in vivo evaluation of formulation of repaglinide with hydroxypropyl- β -cyclodextrin. *Int. J. Pharm* 477, 159–166. <https://doi.org/10.1016/j.ijpharm.2014.10.038> <https://doi.org/>.
- Liao, R.Q., Zhao, Y.L., Liao, X.L., Liu, M.S., Gao, C.Z., Yang, J., Yang, B., 2015. Folic acid-polyamine- β -cyclodextrin for targeted delivery of scutellarin to cancer cells. *Poly. Adv Technol* 26, 487–494. <https://doi.org/10.1002/pat.3477> <https://doi.org/>.
- Ma, X.L., Liao, Z.X., Zhang, Y.L., Chen, Y.Z., 2000. Study of the Podophyllotoxin/ β -Cyclodextrin Inclusion Complex. *J. Inclusion Phenom. Macrocyclic. Chem* 36, 335–342. <https://doi.org/10.1023/A:1008199827029> <https://doi.org/>.
- Na, K., Lee, T.B., Park, K.H., Shin, E.K., Lee, Y.B., Choi, H.K., 2003. Self-assembled nanoparticles of hydrophobically-modified polysaccharide bearing vitamin H as a targeted anticancer drug delivery system. *Eur. J. Pharm. Sci.* 18, 165–173. [https://doi.org/10.1016/S0928-0987\(02\)00257-9](https://doi.org/10.1016/S0928-0987(02)00257-9) <https://doi.org/>.
- Park, K.H., Kang, D.M., Na, K., 2006. Physicochemical Characterization and Carcinoma Cell Interaction of Self-Organized Nanogels Prepared from Polysaccharide/Biotin Conjugates for Development of Anticancer Drug Carrier. *J. Microbiol. Biotechnol.* 16, 1369–1376.
- Periasamy, R., KothaiNayakia, S., Sivakumarb, K., Ramasamy, G., 2020. Synthesis and characterization of host-guest inclusion complex of β -cyclodextrin with 4,4'-methylenedianiline by diverse methodologies. *J. Mol. Liq.* 316, 113843 <https://doi.org/10.1016/j.molliq.2020.113843> <https://doi.org/>.
- Qiu, N., Li, X.B., Liu, J.D., 2017. Application of cyclodextrins in cancer treatment. *J. Inclusion Phenom. Macrocyclic Chem* 89, 229–246. <https://doi.org/10.1007/s10847-017-0752-2> <https://doi.org/>.
- Qiu, N., Zhao, X., Liu, Q.M., Shen, B.L.S., Liu, J.D., Li, X.B., An, L.Y., 2019. Inclusion complex of emodin with hydroxypropyl- β -cyclodextrin: Preparation, physicochemical and biological properties. *J. Mol. Liq* 289, 111151. <https://doi.org/10.1016/j.molliq.2019.111151> <https://doi.org/>.
- Roy, A., Zhao, Y.C., Yang, Y., Szeitz, A., Klassen, T., Li, S.D., 2017. Selective targeting and therapy of metastatic and multidrug resistant tumors using a long circulating podophyllotoxin nanoparticle. *Biomaterials* 137, 11–22. <https://doi.org/10.1016/j.biomaterials.2017.05.019> <https://doi.org/>.
- Raza, A., Sun, H.F., Bano, S., Zhao, Y.Y., Xu, X.Q., Tang, J., 2017. Preparation, characterization, and in vitro anti-inflammatory evaluation of novel water soluble kamebakaurin/hydroxypropyl- β -cyclodextrin inclusion complex. *J. Mol. Struct.* 1130, 319–326 <https://doi.org/10.1016/j.molstruc.2016.10.059>.
- Sinha, V.R., Anitha, R., Ghosh, S., Nanda, A., Kumria, R., 2005. Complexation of Celecoxib with β -Cyclodextrin: Characterization of the Interaction in Solution and in Solid State. *J. Pharm. Sci.* 94, 676–687. <https://doi.org/10.1002/jps.20287> <https://doi.org/>.
- Siafaka, P.I., Neslihan, Ü.O., Mariza, M., Spyridoula, G., Sevda, E., Eleni, P., Evangelos, K., Dimitrios, N., 2016. Two Different Approaches for Oral Administration of Voriconazole Loaded Formulations: Electrospun fibers versus β -Cyclodextrin Complexes. *Int. J. Mol. Sci* 17, 282. <https://doi.org/10.3390/ijms17030282> <https://doi.org/>.
- Tang, P.X., Li, S.S., Wang, L.L., Yang, H.Q., Yan, J., Li, H., 2015. Inclusion complexes of chlorzoxazone with β - and hydroxypropyl- β -cyclodextrin: Characterization, dissolution, and cytotoxicity. *Carbohydr. Polym* 131, 297–305. <https://doi.org/10.1016/j.carbpol.2015.05.055> <https://doi.org/>.
- Williams, R.O., Mahaguna, V., Sriwongjanya, M., 1998. Characterization of an inclusion complex of cholesterol and hydroxypropyl- β -cyclodextrin. *Eur. J. Pharm. Biopharm* 46, 355–360. [https://doi.org/10.1016/S0939-6411\(98\)00033-2](https://doi.org/10.1016/S0939-6411(98)00033-2) <https://doi.org/>.
- Waleczek, K.J., Cabral-Marques, H.M., Hempel, B., Schmidt, P.C., 2003. Phase solubility studies of pure(-)- α -bisabolol and camomile essential oil with β -cyclodextrin. *Eur. J. Pharm. Bio* 55, 247–251. [https://doi.org/10.1016/S0939-6411\(02\)00166-2](https://doi.org/10.1016/S0939-6411(02)00166-2) <https://doi.org/>.
- Wang, L., Jiang, X.H., Xu, W.J., Li, C.R., 2007. Complexation of tanshinone IIA with 2-hydroxypropyl- β -cyclodextrin: Effect on aqueous solubility, dissolution rate, and intestinal absorption behavior in rats. *Int. J. Pharma* 341, 58–67. <https://doi.org/10.1016/j.ijpharm.2007.03.046> <https://doi.org/>.
- Wei, K.C., Li, J., Chen, G.S., Jiang, M., 2013. Dual Molecular Recognition Leading to a Protein-Polymer Conjugate and Further Self-Assembly. *ACS Macro Let* 2, 278–283. <https://doi.org/10.1021/mz400036t> <https://doi.org/>.
- Wang, R., Zhi, X., Li, J., Xu, H., 2015. Synthesis of novel oxime sulfonate derivatives of 2'-(2', 6')-(di) chloropropodophyllotoxins as insecticidal agents. *J. Agric. Food Chem.* 63, 6668e6674. <https://doi.org/10.1021/acs.jafc.5b02036> <https://doi.org/>.
- Xu, J., Zhang, Y., Li, X., Zheng, Y., 2017. Inclusion complex of nateglinide with sulfobutyl ether β -cyclodextrin: Preparation, characterization and water solubility. *J. Mol. Struct* 1141, 328–334. <https://doi.org/10.1016/j.molstruc.2017.03.116> <https://doi.org/>.
- Yang, B., Lin, J., Chen, Y., Liu, Y., 2009. Artemether/hydroxypropyl- β -cyclodextrin host-guest system: Characterization, phase-solubility and inclusion mode. *Bioorg. Med. Chem* 17, 6311–6317. <https://doi.org/10.1016/j.bmc.2009.07.060> <https://doi.org/>.
- Yao, Y., Xie, Y., Hong, C., Li, G., Shen, H., Ji, G., 2014. Development of a myricetin/hydroxypropyl- β -cyclodextrin inclusion complex: preparation, characterization, and evaluation. *Car. Poly* 110, 329–337. <https://doi.org/10.1016/j.carbpol.2014.04.006> <https://doi.org/>.
- Yu, X., Che, Z., Xu, H., 2017. Recent advances in the chemistry and biology of podophyllotoxins. *Chem. Eur. J.* 23 (19), 4467–4526. <https://doi.org/10.1002/chem.201781961> <https://doi.org/>.
- Yan, C.X., Liang, N., Li, Q., Yan, P.F., Sun, S.P., 2019. Biotin and arginine modified hydroxypropyl- β -cyclodextrin nanoparticles as novel drug delivery systems for paclitaxel. *Car. Poly* 216, 129–139. <https://doi.org/10.1016/j.carbpol.2019.04.024> <https://doi.org/>.